nature neuroscience

Modeling pain *in vitro* using nociceptor neurons reprogrammed from fibroblasts

Brian J Wainger[1–3,8], Elizabeth D Buttermore[1,3,8], Julia T Oliveira[1,4], Cassidy Mellin[1], Seungkyu Lee[1,3], Wardiya Afshar Saber[1], Amy J Wang[1], Justin K Ichida[5,6], Isaac M Chiu[1,3], Lee Barrett[1], Eric A Huebner[1,3], Canan Bilgin[1], Naomi Tsujimoto[5], Christian Brenneis[1], Kush Kapur[1], Lee L Rubin[5], Kevin Eggan[5,7] & Clifford J Woolf[1,3]

Reprogramming somatic cells from one cell fate to another can generate specific neurons suitable for disease modeling. To maximize the utility of patient-derived neurons, they must model not only disease-relevant cell classes, but also the diversity of neuronal subtypes found *in vivo* and the pathophysiological changes that underlie specific clinical diseases. We identified five transcription factors that reprogram mouse and human fibroblasts into noxious stimulus–detecting (nociceptor) neurons. These recapitulated the expression of quintessential nociceptor-specific functional receptors and channels found in adult mouse nociceptor neurons, as well as native subtype diversity. Moreover, the derived nociceptor neurons exhibited TrpV1 sensitization to the inflammatory mediator prostaglandin E2 and the chemotherapeutic drug oxaliplatin, modeling the inherent mechanisms underlying inflammatory pain hypersensitivity and painful chemotherapy-induced neuropathy. Using fibroblasts from patients with familial dysautonomia (hereditary sensory and autonomic neuropathy type III), we found that the technique was able to reveal previously unknown aspects of human disease phenotypes *in vitro*.

Directed differentiation from pluripotent stem cells and lineage reprogramming of fibroblasts can both be used to derive a wide range of different neuronal subtypes[1,2]. Although the known sequence of morphogen exposure and consequent molecular changes in the development of specific neurons can guide directed differentiation strategies, the selection of transcription factors for lineage reprogramming from fibroblasts remains essentially empirical. No single transcription factor has proven to be essential for driving cell fates in all of the neuronal reprogramming studies to date, despite the fact that specific factors such as *Ascl1* or *Ngn2* seem particularly potent in deriving a range of different neuronal subtypes[3]. *Brn2*, *Ascl1* and *Myt1l* (or BAM) generate generic neurons on their own[4] and specific neuronal subtypes when combined with additional factors[5]. Moreover, the developmental stage at which a particular transcription factor acts *in vivo* may determine whether that factor facilitates or inhibits the patterning of reprogrammed neurons[4,5].

Nociceptors are the first-order neurons in the pain sensory transduction pathway and take the critical initial step in the detection of noxious stimuli (nociception) and the development of inflammatory and neuropathic pain[6,7]. Nociceptor neurons employ a host of highly specific ionotropic receptors and ion channels, including TrpV1, TrpA1, TrpM8 and P2X3 receptors to transduce stimuli, and slow, tetrodotoxin (TTX)-resistant sodium channels ($Na_V1.8$ and $Na_V1.9$) that generate their characteristic broad action potentials[8]. Efforts to derive nociceptors using a small molecule–based directed differentiation strategy from human neural crest precursors have produced neurons that recreate some, but not all, of these characteristic receptors and channels[9].

Mutations in nociceptor-specific membrane proteins underlie a wide range of pain diseases, including rare, but severe, channelopathies resulting from $Na_V1.7$ or TrpA1 mutations[10], common small fiber neuropathies resulting from activating mutations in $Na_V1.7$ or $Na_V1.8$ (refs. 11,12), as well as a variety of pain-predisposing polymorphisms[13,14]; however, the biological effects of these mutations on nociception have not been studied in human sensory neurons. Nociceptors normally activate only following intense, potentially damaging stimuli to provide a protective warning of imminent tissue injury. However, they also have the notable capacity to become sensitized after exposure to inflammatory mediators[15,16] or by chemotherapeutic drugs[17], resulting in a reduced activation threshold so that innocuous stimuli can generate a pain response. Pain hypersensitivity can have a physiologically useful role in minimizing further injury and in promoting healing once damage has occurred; however, such transient sensitization, when it persists, promotes the development of chronic pain.

Nociceptor neuron development occurs through dorsalization in the neural tube[18], followed by neural crest induction and migration[19],

[1]F.M. Kirby Neurobiology Center, Boston Children's Hospital and Harvard Stem Cell Institute, Cambridge, Massachusetts, USA. [2]Department of Anesthesia, Critical Care and Pain Medicine and Department of Neurology, Massachusetts General Hospital, Boston, Massachusetts, USA. [3]Department of Neurobiology, Harvard Medical School, Boston, Massachusetts, USA. [4]Laboratório de Neurodegeneração e Reparo, Departamento de Patologia, Faculdade de Medicina, Universidade Federal Do Rio De Janeiro, Rio de Janeiro, Brazil. [5]Harvard Stem Cell Institute, Department of Stem Cell and Regenerative Biology, Harvard University, Cambridge, Massachusetts, USA. [6]Department of Stem Cell Biology and Regenerative Medicine, Eli and Edythe Broad CIRM Center for Regenerative Medicine and Stem Cell Research, University of Southern California, Los Angeles, California, USA. [7]The Howard Hughes Medical Institute, Harvard University, Cambridge, Massachusetts, USA. [8]These authors contributed equally to this work. Correspondence should be addressed to C.J.W. (clifford.woolf@childrens.harvard.edu).

Received 31 July; accepted 29 October; published online 24 November 2014; corrected online 10 December 2014 (details online); doi:10.1038/nn.3886

and then nociceptor specification in the still-multipotent neural crest lineage[20]. The generation of nociceptor progenitors expressing the TrkA neurotrophin receptor (*Ntrk1*) and postnatal nociceptors expressing TrpV1 requires the basic helix-loop-helix transcription factor *Ngn1* (Neurogenin1), which is normally present from approximately E9–13 in the embryonic mouse[21]. Although developing nociceptors express multiple Trk-family receptors, maturing nociceptors express only TrkA. Brn3a (*POU4F1*) promotes *Runx1* expression, which, together with *Isl1* (Islet 1) and *Klf7*, maintains TrkA expression in developing nociceptors[22–25]. A subset of nociceptors that become the peptidergic subclass of nociceptors maintain TrkA expression and express calcitonin gene–related peptide (CGRP, *CalcA*) and substance P. For non-peptidergic nociceptors, most of which bind isolectin B4, the glial cell–derived neurotrophic factor (GDNF) receptor Ret replaces TrkA in a process dependent on Runx1, and the loss of Runx1 markedly reduces TrpV1 expression[23].

We set out to produce nociceptor neurons through transcription-mediated lineage conversion of fibroblasts. From an initial set of 12 factors, we found that expressing five factors was sufficient to generate functional mouse nociceptor neurons. In a direct comparison between the induced nociceptors and primary adult mouse nociceptors, we found that the induced neurons mimicked bona fide nociceptors with regard to the function of the specific individual receptors and channels, such as TrpA1, TrpM8, P2X3 and $Na_V1.8$, as well as with regard to the population diversity. The induced neurons also modeled inflammatory peripheral sensitization, a critical process that underlies transient pain hypersensitivity and contributes to the pathological transition to chronic pain, as well as sensitization following exposure to the chemotherapeutic drug oxaliplatin. Finally, we derived human nociceptor neurons from patients with familial dysautonomia (FD); these neurons revealed potentially disease-relevant phenotypes *in vitro*.

RESULTS

Selection and optimization of transcription factors

We first developed nociceptor reporter mice by taking advantage of an existing *Trpv1-Cre* driver[26] and *loxP*-flanked *tdTomato* mice to generate *Trpv1-Cre*$^{+/-}$::*tdTomato*$^{+/-}$ reporter mice, from which we obtained mouse embryonic fibroblasts (MEFs). Activation of the tdTomato reporter signaled the conversion of the MEFs to TrpV1-expressing cells (**Supplementary Fig. 1**). We began with nine transcription factors that were selected to promote lineage conversion to nociceptors in combination with the three BAM factors (12 total; **Table 1**). These factors were chosen using a combination of previous studies, transcription factor expression profiles in FACS-sorted adult mouse nociceptors ($Na_V1.8$ positive) as compared with proprioceptors (parvalbumin positive) (Chiu, I.M., Barrett, L.B., Williams, E., Strochlic, D.E., Lee, S. *et al.*, unpublished data), an expression profile similarity to $Na_V1.8$ in the BioGPS database[27], and postnatal dorsal root ganglion (DRG) expression in the Allen Brain Atlas[28].

As expected, there was no baseline activation of the tdTomato reporter in MEFs (data not shown). Staining of MEFs for neuronal precursor markers using antibodies to Nestin, Sox1 and Ki67, as well as for neuron-specific class III β-tubulin (Tuj1), was negative in each case (**Supplementary Fig. 2**). After transducing the fibroblasts with a combination of all 12 individual retroviruses containing the selected transcription factors, we detected a small number of tdTomato-positive cells with a neuronal morphology after 2 weeks (**Supplementary Fig. 3a**). To identify those transcription factors that were either critical for or inhibitory to lineage reprogramming into TrpV1-expressing cells, we then sequentially eliminated each factor, one at a time. To our surprise, the omission of some transcription factors strongly supported by the literature as having a role in promoting TrpV1 expression, such as *Runx1*, did not eliminate TrpV1 reporter expression (**Supplementary Fig. 3b**). In fact, omission of Brn3a led to a marked increase in the number of tdTomato-positive cells (**Supplementary Fig. 3c**). We identified from this iterative process three factors that were critical to the TrpV1 lineage reprogramming process in that their omission led to a near complete absence of tdTomato and neuronal class III β-tubulin (Tuj1)-positive cells bearing a neuronal morphology: *Ascl1*, *Myt1l* and *Klf7* (**Supplementary Fig. 3d–f**).

When we combined the three BAM factors with *Isl2*, *Ngn1* and *Klf7*, we again observed only a small number of tdTomato- and Tuj1-positive cells (**Fig. 1a**). Because prior studies[5] and our initial drop out experiments detected specific factors that could inhibit the lineage reprogramming process, we performed single factor dropouts from these six factors and found that omission of *Brn2* led to a marked increase in the number of tdTomato-positive neurons (**Fig. 1b**), giving a yield of approximately 14% of plated fibroblasts that were both tdTomato and Tuj1 positive (less than 0.1% were tdTomato positive and Tuj1 negative). Removal of any other factor from the six sharply reduced the number of tdTomato-positive neurons (**Fig. 1c–h**). Next, we evaluated *Ngn1* alone and in combination with the BAM factors; however, the yield was much lower than with the optimized five factor combination (**Supplementary Fig. 4**). Indeed, further removal of any of the five factors resulted in a marked decrease in tdTomato- and Tuj1-positive cells (**Supplementary Fig. 5**).

Molecular characterization of induced mouse nociceptors

To determine whether tdTomato-positive reprogrammed neurons phenocopied bona fide nociceptors, we evaluated the expression of protein markers specific for nociceptor neurons. Nearly all tdTomato-positive neurons stained for the pan-neuronal marker Tuj1 and had a neuronal-like morphology with many long branching axons, and most Tuj1-positive neurons were also tdTomato positive (**Fig. 2a**). Staining with an antibody to TrpV1 confirmed the translation of the TrpV1 protein in the vast majority of tdTomato-positive neurons

Table 1 Candidate transcriptions factors for lineage conversion to nociceptor neurons

Gene	Source	Family	Role in reprogramming/sensory system
Ascl1	Lit	Basic helix-loop-helix, achaete-scute	Neuronal lineage reprogramming[4]
Drgx (*Drg11*)	Lit	Helix-turn-helix, paired box	Survival of peptidergic and non-peptidergic nociceptors[48]
Ebf1	Exp	Zinc finger	Downstream of Ngn[49]
Etv1	Exp	Helix-turn-helix, tryptophan clusters	Proprioceptive marker[24]
Isl2	Exp, BioGPS	Homeodomain, LIM region	Unknown
Klf7	Lit, Exp, BioGPS	Zinc finger, Krueppel like	TrkA maintenance[25]
Myt1L	Lit	Zinc finger	Neuronal lineage reprogramming[4]
Ngn1	Lit	Basic helix-loop-helix	TrkA and subsequent TrpV1 expression[21]
Pknox2	Exp	Homeodomain, TALE	Unknown
Pou4f1 (*Brn3a*)	Lit	Homeodomain, POU (Class IV)	Neuronal lineage reprogramming[4]
Runx1	Lit	β-scaffold, Runt	Non-peptidergic identify and TrpV1 expression[23]
Tlx3	Lit	Helix-turn-helix, homeodomain	Glutamatergic identity[50]

Lit, literature; Exp, transcriptome of sorted nociceptors compared with proprioceptors; BioGPS[27].

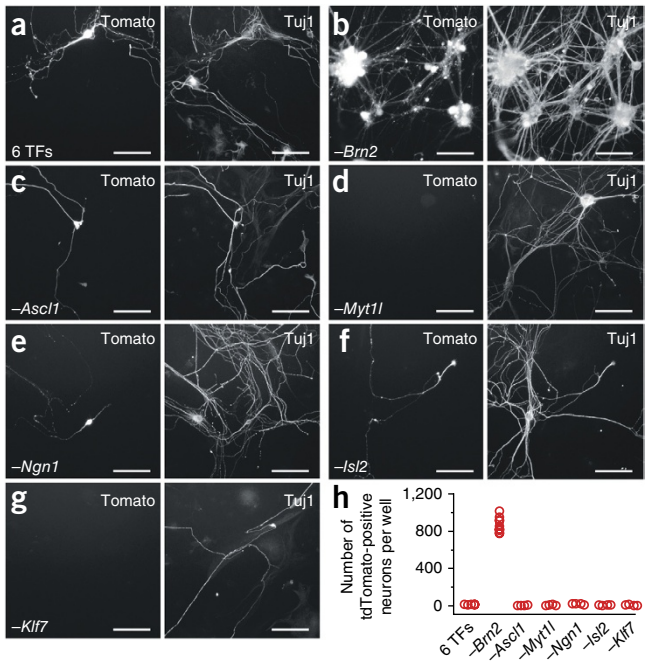

Figure 1 Combinations of transcription factors result in nociceptor production. (**a**) Few tdTomato-, Tuj1-positive neurons were produced by the combination of six factors (6 TFs): *Brn2*, *Ascl1*, *Myt1l*, *Ngn1*, *Isl2* and *Klf7*. (**b**) Removal of *Brn2* markedly increased the number of tdTomato-, Tuj1-positive neurons. (**c**–**g**) Omission of *Ascl1* (**c**), *Myt1l* (**d**), *Ngn1* (**e**), *Isl2* (**f**) or *Klf7* (**g**) from the six factors disrupted the generation of nociceptor neurons. Representative images for each transcription factor drop out were taken from $n = 4$ wells from two separate transductions. Scale bars represent 100 µm. (**h**) Quantification of the single factor dropout studies from $n = 4$ wells from each of two separate independent transductions for each category.

(**Fig. 2b**). In mouse DRG, most TrpV1-expressing neurons are C fibers that express the marker peripherin (*Prph*)[29], whereas only a small percentage of A-δ fibers are also TrpV1 positive[26]. In the induced neurons, a majority of tdTomato-positive neurons expressed peripherin (66.9 ± 4.1%, $n = 16$ wells from 4 separate transductions; **Fig. 2c**) and many expressed CGRP (22.3 ± 6.6%, $n = 4$ wells from 2 separate transductions; **Fig. 2d**); however, a smaller number of cells stained for the intermediate filament NF200, a marker of myelinated A-δ nociceptors in this context (**Fig. 2e**). In contrast, the derived nociceptors did not stain for smooth muscle actin (SMA), a marker of muscle, despite reports of TrpV1 expression in muscle[30] (**Supplementary Fig. 6a**,**b**). Furthermore, neurons derived from the three BAM factors did not express nociceptor markers, consistent with their high specificity (**Supplementary Fig. 6c**–**g**).

Because specific antibodies do not exist for many quintessential nociceptor proteins, we used quantitative RT-PCR to compare nociceptor marker mRNA levels in tdTomato-positive induced nociceptors and tdTomato-positive adult mouse nociceptors relative to levels in MEFs (**Fig. 2f**). For this analysis, we used patch pipettes to pick tdTomato-positive induced and primary mouse neurons, as well as MEFs, and plotted the levels of specific transcripts in induced and primary nociceptors relative to MEFs. The fibroblast marker *S100a4* was expressed at a similar very low level in both the induced and primary nociceptors, consistent with a non-fibroblast identity of the induced nociceptors. $Na_V1.7$ (*Scn9a*), which is found in nociceptor and autonomic peripheral neurons, was present in both the induced and primary nociceptors, as was TrkA (*Ntrk1*), which is turned on in developing nociceptors and persists in the peptidergic subset of mature nociceptors, although the expression of $Na_V1.7$ and TrkA in the induced neurons was several fold less than that in the primary DRGs. Together, these immunohistochemistry and PCR data suggest that the induced neurons express a complement of bona fide nociceptor-specific markers.

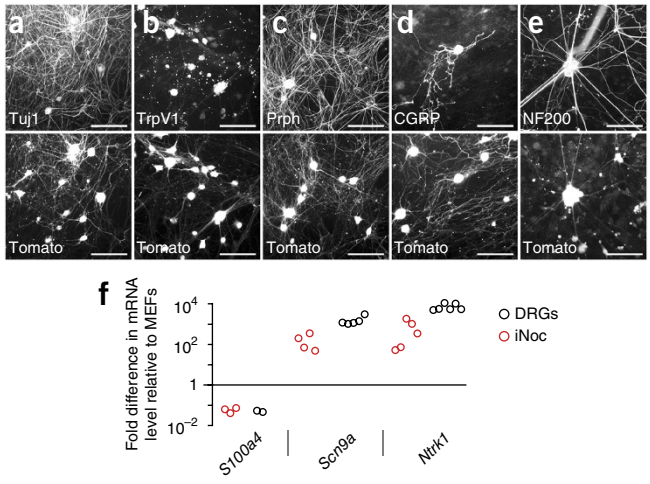

Figure 2 Induced nociceptors (iNoc) express characteristic nociceptor genes. (**a**,**b**) Tuj1 (**a**) and TrpV1 (**b**) expression in fibroblast-derived nociceptor neurons. (**c**) Most induced nociceptors expressed the C-fiber marker peripherin (Prph). (**d**) A number of induced nociceptors expressed the peptidergic-marker CGRP. (**e**) A small number of induced nociceptors expressed the intermediate filament marker NF200 found in myelinated fibers. Representative images were selected from immunostaining that was repeated in $n = 4$ wells from two independent transductions. Scale bars represent 100 µm. (**f**) Quantitative RT-PCR data showing expression levels of nociceptor-specific genes in 50 picked tdTomato-positive primary adult mouse nociceptors (DRGs, black circles) and 50 picked tdTomato-positive induced nociceptors (red circles), relative to their levels in MEFs, from a minimum of two independent biological replicates (biological replicates represented as independent circles).

Functional properties of induced mouse nociceptors

To investigate the functional properties of the induced nociceptors, we performed calcium imaging with a battery of agonists and evaluated the number of responders in the tdTomato-positive population with a stable baseline and response to KCl (which activates voltage-gated calcium channels through depolarization and serves as a measure of neuronal functional integrity; **Fig. 3a**). We chose concentrations of agonists for TrpM8 (250 µM menthol), TrpA1 (100 µM mustard oil) and TrpV1 (1 µM capsaicin) that only activated their respective cognate receptors[31]. We found that 39% of the cells responded to capsaicin, 9% to mustard oil and 3% to menthol ($n = 227$ tdTomato-positive cells that responded to KCl; **Fig. 3a**,**b**). There were occasional cells that responded to both mustard oil and capsaicin, a single cell that responded to menthol and mustard oil, but not capsaicin, and one cell that responded to all three agonists. We did not observe any tdTomato-positive cells that responded to menthol alone, but we did identify a small number of tdTomato-negative cells that responded to menthol, but not the other Trp agonists (**Supplementary Fig. 7a**). In contrast, none of the 50 KCl-responding neurons derived from the BAM factors alone responded to capsaicin (data not shown). Using the same experimental procedure, we then asked how the frequencies of the different combinations of receptors in individual neurons compared between induced nociceptors and adult mouse nociceptors.

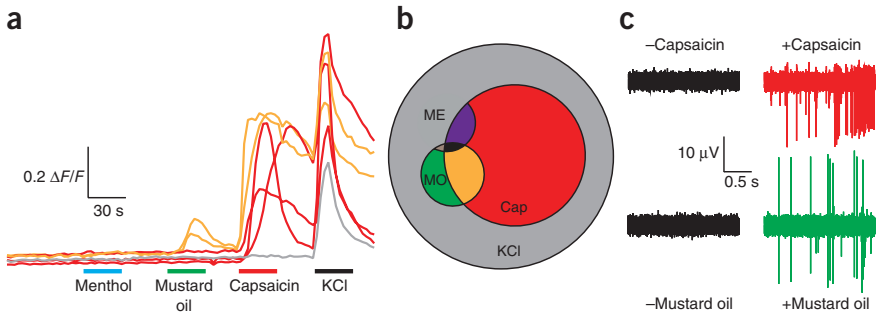

Figure 3 Induced neurons respond to different Trp channel agonists. (**a**) Sample calcium-imaging responses to sequential application of menthol (250 μM), mustard oil (100 μM), capsaicin (1 μM) and KCl (40 mM) in a single dish of induced tdTomato-positive–derived nociceptors. Traces are representative recordings from $n = 227$ tdTomato-positive, KCl-responding cells cultured in 19 dishes from 3 independent transductions. (**b**) Venn diagram showing subgroups of tdTomato-positive cells that responded to KCl (40 mM, gray), capsaicin (Cap, 1 μM, red, 39%), mustard oil (MO, 100 μM, lower small circle, green, 9%) and menthol (ME, 250 μM, upper small partial circle, blue, 3%; note that none of the tdTomato-positive cells responded to menthol alone). (**c**) Sample electrodes from extracellular MEA recordings of induced neurons before (left) and after (right) the application of capsaicin (1 μM, upper) and mustard oil (100 μM, lower). Sample recordings for each agonist are indicative of results from three experiments across two independent transductions, in which all replicates showed an increase in firing after agonist application.

In tdTomato-positive primary DRG neurons dissected and cultured from adult *Trpv1*$^{+/-}$::*tdTomato*$^{+/-}$ mice, we found that 36% of the neurons responded to capsaicin, 2.5% to mustard oil and 2.5% to menthol (n = 249 tdTomato-positive cells that responded to KCl; **Supplementary Fig. 7b**,**c**). Thus, the nociceptor lineage reprogramming not only yielded physiologically functional TrpV1, TrpA1 and TrpM8 proteins in the induced neurons, but the frequencies and combinations of the different receptors in the induced neurons closely mimicked those of adult mouse nociceptors.

Although calcium imaging provides detailed information about calcium entry through Trp channels, it does not evaluate whether activation of these channel evokes action potential firing in the neurons. By culturing the induced neurons on extracellular multi-electrode arrays (MEAs), we found that both capsaicin and mustard oil application evoked robust action potential firing from the induced neurons (three of three arrays for capsaicin and three of three arrays for mustard oil; **Fig. 3c**).

We next used whole-cell patch-clamp recordings to define the electrophysiological properties of the induced nociceptors and found that capsaicin (1 μM) elicited inward currents in 6 of 11 tdTomato-positive induced neurons, consistent with, but somewhat higher than, the calcium imaging results (**Fig. 4a**). The P2X3 subtype of ionotropic purinergic receptors is expressed specifically in nociceptor neurons[32]. Application of the P2X3-specific agonist α,β-methylene-ATP (30 μM) elicited rapidly-adapting inward currents in 8 of 16 neurons (**Fig. 4b**) that were blocked completely by A-397491, a specific P2X3 antagonist, in four of four neurons (data not shown)[33].

Perhaps the most nociceptor-specific functional marker is the TTX-resistant $Na_V1.8$ sodium channel, which produces a portion of the current in the nociceptor action potential upstroke[34]. In voltage clamp, we found that depolarizing voltage steps elicited inward sodium currents both before and after the application of 300 nM TTX (14 of 15 recorded induced nociceptors had TTX-resistant sodium currents greater than 50 pA; **Fig. 4c**). Consistent with our expression studies, the slow channel kinetics of the TTX-resistant currents are typical for $Na_V1.8$ as opposed to the fast $Na_V1.5$ cardiac sodium channel, which is present in developing embryonic nociceptors[35]. Furthermore, 5 of 14 neurons with TTX-resistant sodium currents also exhibited a persistent sodium component, which previous studies have found to be a result of $Na_V1.9$ (**Fig. 4c**)[34,36]. The ability to generate action potentials in the presence of TTX is a feature of nociceptors, but not of other DRG or central neurons. The induced neurons fired single TTX-resistant action potentials that overshot 0 mV in 7 of 12 neurons (**Fig. 4d**). $Na_V1.8$ is responsible for the characteristic broad action potential shape of the nociceptor action potential[8], which we found to be a property of the induced neurons (mean action potential width of 3.32 ± 0.33 ms, n = 13 cells); as expected, adult primary tdTomato-positive nociceptors fired broad action potentials, but large tdTomato-negative primary non-nociceptor DRG neurons did not (**Fig. 4e**). In addition to differences in action potential morphology,

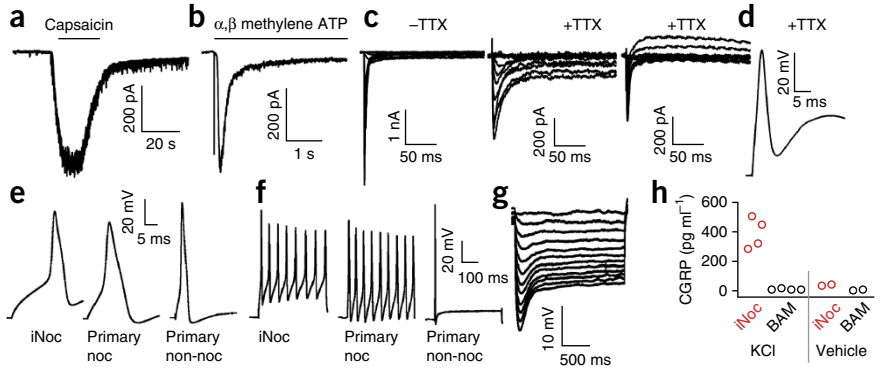

Figure 4 Whole-cell patch-clamp recordings of tdTomato-positive induced nociceptors. (**a**) Current recording in response to treatment with 1 μM capsaicin (6 of 11 induced neurons responded). (**b**) Current recording following the application of 30 μM α,β-methylene-ATP (8 of 16 induced neurons responded). (**c**) Inward currents following step depolarization before (left) and after (middle) the application of 300 nM tetrodotoxin (TTX) (14 of 15 induced neurons had TTX-resistant sodium currents greater than 50 pA). Right, a different neuron without a persistent TTX-resistant sodium current. (**d**) Action potential firing elicited by depolarizing current in the presence of 300 nM TTX (7 of 12 cells fired single TTX-resistant action potentials with peak greater than 0 mV). (**e**,**f**) Examples of individual action potentials (**e**) and trains (**f**) elicited from induced nociceptors (iNoc), tdTomato-positive primary adult nociceptors (primary noc) and tdTomato-negative primary adult non-nociceptors (primary non-noc) (12 of 13 induced neurons fired tonically). (**g**) Examples of sag depolarizations in response to hyperpolarizing current injections in induced nociceptors (11 of 17 induced neurons produced a sag depolarization). (**h**) CGRP was released from induced nociceptors (5F), but not BAM-derived neurons, in response to KCl (80 mM), but not vehicle. Mean (s.e.m.) for induced nociceptors and BAM following KCl stimulation were 390.4 (52.5) and 10.3 (2.6) pg ml^{-1} (n = 4 separate dishes, Mann-Whitney U test, P = 0.03).

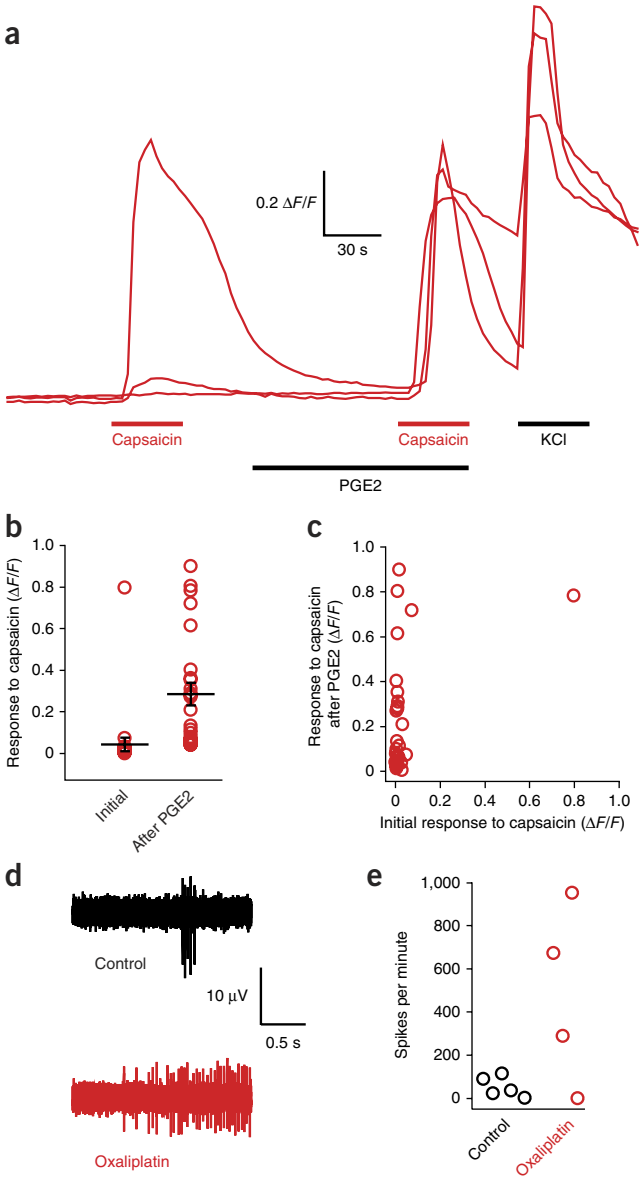

Figure 5 Sensitization of induced nociceptors treated with the inflammatory mediator PGE2 and the chemotherapeutic drug oxaliplatin. (**a**) Sample calcium-imaging recordings of induced nociceptors treated with 300 nM capsaicin before and after treatment with 1 μM PGE2 from recordings of $n = 41$ tdTomato-positive, KCl-responding cells. (**b**) Plot of individual and mean response amplitudes for initial and PGE2-sensitized capsaicin treatments (paired t test, $P = 1.5 \times 10^{-4}$). Error bars represent ±s.e.m. (**c**) Plot of initial versus PGE2-sensitized capsaicin response amplitudes for individual induced neurons. (**d**) Sample traces from extracellular MEA recordings of induced neurons in response to 300 nM capsaicin following a 10-min exposure to vehicle control ($n = 5$ MEAs) or oxaliplatin (50 μM, $n = 4$ MEAs) on induced neurons from two separate transductions. (**e**) Quantification of spikes per minute from induced nociceptors in response to capsaicin alone (control) and capsaicin following oxaliplatin treatment.

the firing pattern of nociceptor neurons to prolonged depolarizing currents is tonic compared with the phasic firing of most large A-β DRG neurons[37]. Induced nociceptors fired tonic action potential trains in response to depolarizing current steps in 12 of 13 cells, consistent with the tonic firing found in tdTomato-positive adult primary mouse nociceptors, and in contrast with the single action potentials elicited in non-nociceptor, large tdTomato-negative adult DRG neurons (**Fig. 4f**).

Although hyperpolarization-activated cyclic nucleotide–sensitive (HCN) currents are not specific for nociceptor neurons, they have an important role within these cells in neuropathic and inflammatory pain[38], and their presence may be important for disease modeling. We found that the induced nociceptors produced typical sag depolarizations in response to hyperpolarization (**Fig. 4g**) in 11 of 17 tdTomato-positive induced neurons, consistent with ZD7288-sensitive HCN currents recorded in voltage clamp (two of two neurons, data not shown).

A critical function of peptidergic neurons, most of which express TrpV1 (ref. 7), is to release neuropeptides such as CGRP and substance P. To assess the fidelity of the induced nociceptors in this capacity, we measured CGRP levels in supernatant following a depolarizing stimulus and found that induced nociceptors, but not BAM-derived neurons, released CGRP after KCl stimulation ($n = 4$ separate dishes, Mann-Whitney U test, $P = 0.03$; **Fig. 4h**). The concentrations of CGRP released by the induced neurons were comparable to those released by primary DRG neurons (**Supplementary Fig. 8**), indicating that the induced neurons have synaptic vesicle release mechanisms in place.

Induced nociceptors model inflammatory sensitization

The transition from high-threshold baseline nociception to low-threshold clinical pain hypersensitivity commonly involves peripheral sensitization of nociceptors. For the induced nociceptors to be valuable *in vitro* models of *in vivo* pathophysiology, they must replicate not only the specific functional channels and receptors of the cells, but also the process of sensitization that leads to pathological pain. Prostaglandin E2 (PGE2) activates the PKA pathway and sensitizes the TrpV1 receptor, reducing its threshold and decreasing desensitization[15,16]. In the tdTomato-positive induced neurons, a low concentration (300 nM) of capsaicin rarely yielded a large response (mean change in fluorescence absorption ratio of $0.028 \pm 3.0 \times 10^{-3}$; **Fig. 5a**,**b**). However, after treatment with PGE2 (1 μM) for 2 min, a second identical capsaicin (300 nM) application yielded a mean response of $0.18 \pm 6.0 \times 10^{-3}$ ($n = 41$ cells, paired t test, $P = 1.5 \times 10^{-4}$). Plotting the magnitudes of the initial capsaicin and PGE2-sensitized capsaicin responses revealed that, although the majority of neurons exhibited small or undetectable initial responses to capsaicin, they produced robust signals after PGE2 sensitization (**Fig. 5c**).

TrpV1 sensitization also may contribute to painful chemotherapy-induced neuropathy due to oxaliplatin[17]. Using MEA recording, we compared capsaicin responses in induced nociceptors treated with either 50 μM oxaliplatin or vehicle control, and found marked sensitization in the oxaliplatin-treated nociceptors (**Fig. 5d**,**e**).

Induction of human nociceptors

To derive nociceptors from human fibroblasts, we initially included *NEUROD1* in the nociceptor induction protocol, as this transcription factor was important in prior human lineage reprogramming studies[39]. However, we found that the reprogramming efficiency was greater without NeuroD1 (five factors) than with NeuroD1 (six factors) (20.7 ± 1.4 Tuj1-positive neurons per field for five factors, 9.7 ± 1.1 for six factors, $n = 6$ wells per group, t test, $P = 1.0 \times 10^{-4}$; **Supplementary Fig. 9**). Furthermore, more neurons exhibited larger sodium currents without NeuroD1 (67% of patched five factor neurons had peak transient sodium currents greater than 500 pA versus 29% of six factor neurons), and five factor neurons were healthier (resting $V_m = -49.3 \pm 2.2$ mV, $n = 33$ five factor neurons; $V_m = -37.3 \pm 3.2$, $n = 20$ six factor neurons; Mann-Whitney U test, $P = 0.001$).

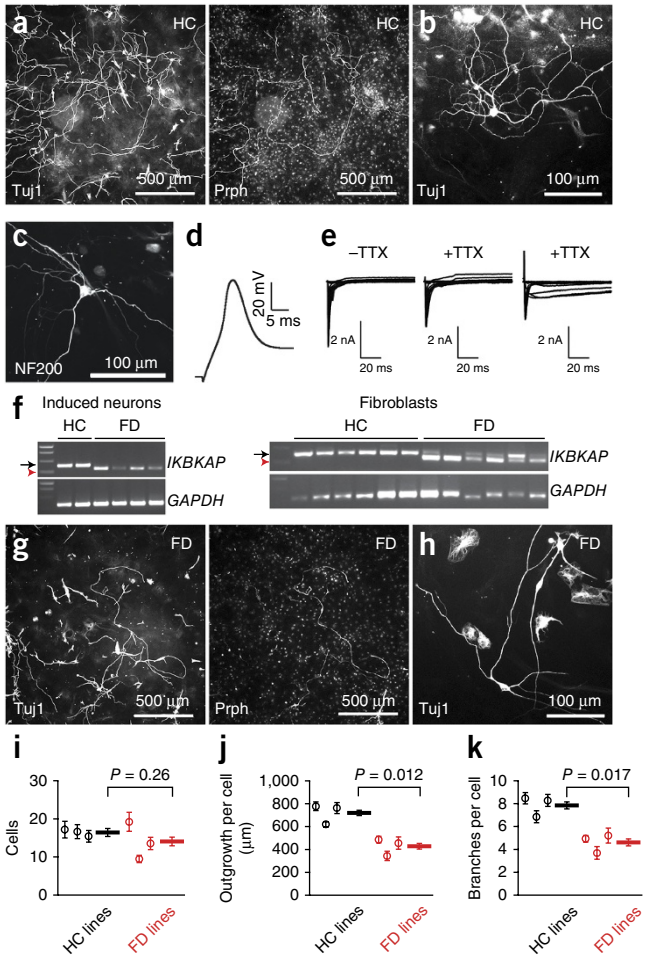

Figure 6 Human fibroblast–derived neurons for human disease modeling. (**a**) Low magnification of Tuj1 (left) and peripherin (Prph, right) staining of HC-derived neurons. Scale bars represent 500 µm. (**b**) High magnification of Tuj1 staining of HC-derived neurons. Scale bar represents 100 µm. (**c**) NF200-positive cell derived from HC fibroblasts. (**d**) Current recording of an action potential from a HC-derived neuron (17 of 33 induced neurons with peak Na current > 500 pA fired at least one action potential with peak greater than 0 mV). (**e**) Total (left) and TTX-resistant (middle) sodium currents from a single HC-derived neuron. Right, persistent TTX-resistant sodium current recordings from a separate HC-derived neuron characteristic of $Na_V1.9$. (**f**) RT-PCR for *IKBKAP* and *GAPDH* from single human induced neurons (left) and single human fibroblasts (right) showed normal (black arrow) and abnormally spliced (red arrowhead) transcripts. Full-length gels are presented in **Supplementary Figure 10**. (**g**) Low magnification of Tuj1 (left) and peripherin (right) staining of neurons derived from a patient with FD. Scale bars represent 500 µm. (**h**) High magnification of Tuj1 staining of FD-derived neurons. Scale bar represents 100 µm. For all images, representative images were selected from human neurons generated in $n = 6$ wells from three separate transductions. (**i**) Quantification of Tuj1-positive neurons in HC- and FD-derived nociceptors (random intercept mixed-effects model, $P = 0.26$). (**j**) Neurite outgrowth per cell for HC- and FD-derived Tuj1-positive nociceptors (random intercept mixed effects model, $P = 0.012$). (**k**) Number of branches per cell for HC- and FD-derived Tuj1-positive nociceptors (random intercept mixed effects model $P = 0.017$). For **i**–**k**, images were analyzed from three pairs of age-matched HC and FD patient lines from each of three separate transductions ($n = 20$ wells per line). Error bars represent ±s.e.m.

Using healthy control (HC) subject fibroblasts, we found that the five factors yielded Tuj1-positive neurons at an efficiency of 5% of plated fibroblasts, and that 16% of the Tuj1-positive neurons also expressed peripherin (**Fig. 6a**,**b**); these efficiencies were somewhat lower than those of the mouse induced nociceptors. A small number of the Tuj1-positive neurons were NF200 positive (**Fig. 6c**). We recorded from the neurons using whole-cell patch clamp. Although we did not have a reporter for a particular neuronal subtype, the induced human neurons fired broad action potentials (mean action potential width = 3.88 ± 0.41 ms, $n = 17$ neurons; **Fig. 6d**), consistent with functional nociceptors. In 38 voltage-clamp recordings, we applied TTX to neurons with a large total sodium current (greater than 1 nA) and detected TTX-resistant sodium currents in ten of ten neurons (**Fig. 6e**). As in both our mouse induced nociceptors and primary mouse and human nociceptors[34,36], the induced human neurons had different combinations of slow and persistent TTX-resistant sodium currents, consistent with $Na_V1.8$ and $Na_V1.9$ contributions, respectively (**Fig. 6e**).

To evaluate the potential of the human neurons for disease modeling, we reprogrammed fibroblasts from three HCs and three unrelated, age-matched subjects with familial dysautonomia (FD, hereditary sensory and autonomic neuropathy type III, Riley-Day syndrome) resulting from a homozygous donor splice site mutation that results in deletion of intron 20 from the I-κ-β kinase complex-associated protein (*IKBKAP*) RNA[40]. We found that single FD-derived neurons picked using patch pipettes exclusively expressed the abnormally spliced transcript, something not previously identified, whereas the HC-derived neurons expressed only the normal transcript (**Fig. 6f**). FD fibroblasts expressed a mixture of abnormally spliced and normal transcripts, consistent with prior studies[41,42], whereas HC fibroblasts expressed only the normal transcript (**Fig. 6f** and **Supplementary Fig. 10**).

Although we detected peripherin-positive, Tuj1-positive neurons from all HC and FD subjects (**Fig. 6g**,**h**), the number of neurons was decreased in FD subjects (16.5 ± 1.1 HC neurons per well, $n = 60$ wells; 14.1 ± 1.1 FD neurons per well, $n = 60$ wells; difference between HC neurons per well and FD neurons per well = 2.3 ± 1.5, $n = 60$ wells; random intercept mixed-effects model, $P = 0.26$; **Fig. 6i**) and we observed a robust reduction in neurite outgrowth per cell (725 ± 24 µm per HC neuron, $n = 60$ wells; 433 ± 25 µm per FD neuron, $n = 60$ wells; difference between HC neuron outgrowth per cell per well and FD neuron outgrowth per cell per well = 291.3 ± 32.6 µm, $n = 60$ wells; random intercept mixed-effects model $P = 0.012$; **Fig. 6j**), as well as in the number of branches per neuron (7.9 ± 0.3 branches per HC neuron, $n = 60$; 4.7 ± 0.3 branches per FD neuron, $n = 60$ wells; difference between HC braches per neuron per well and FD branches per neuron per well = 3.3 ± 0.4, $n = 60$ wells; random intercept mixed-effects model, $P = 0.017$; **Fig. 6k**) compared with HC-derived neurons.

DISCUSSION

The subjective nature of pain as a human experience confounds its clinical study, raises questions about the relevance of animal models and complicates the development of effective treatments[43]. Furthermore, limited physiological studies of primary human nociceptors highlight differences between human and rodent nociceptors, including the function of individual channels and receptors as well as their distribution in different nociceptor subtypes[44], thereby emphasizing the importance of investigating human nociception using human nociceptors. Modeling key mechanistic aspects of human pain processing with derived human cells may enable phenotypic screens for analgesics based on basal and sensitized neurons from chronic pain subjects. Such approaches would improve on current drug screens that employ heterologously expressed targets in

non-neuronal cells and consequently do not reflect the native scaffolding and molecular signaling present in human neurons, the pathophysiological changes that drive clinical pain and genetic backgrounds that may increase pain susceptibility.

We found that a small number of transcription factors can quite efficiently convert fibroblasts into neurons that express the key specific functional receptors found in bona fide adult nociceptors. Although TrpV1 is expressed in a tiny fraction of central neurons[30], $Na_V1.8$ and TrpA1 are not expressed in the CNS. The collective expression of subsets of these markers defines specific subpopulations[7], and, to a first approximation, our neurons recreated the combinatorial patterns that define the diversity of TrpV1-expressing nociceptive neuronal cohorts found in primary mouse nociceptors. Notably, we seemed not to have derived a single nociceptor type, but instead engineered multiple subtypes of cells with properties and frequencies similar to those found *in vivo*. Three possible explanations will need to be investigated in future studies. First, there may be an autonomous program driving the native lineage diversity that is replicated by our transcription factors. Second, non-cell autonomous communication among neurons could influence their identity. Third, different identities could reflect different relative levels of transcription factor expression.

Although the transcription factor combinations that facilitate induction of specific fates have typically incorporated factors known to have defined roles in the development of those neurons[1], some of the factors that we used do not have any well-defined developmental role. We chose Isl2 because of its strong differential expression in FACS-sorted nociceptors compared with proprioceptors and an expression pattern similarity to $Na_V1.8$ (ref. 27), although nothing is known about its role in nociceptor development. Notably, the *in situ* expression of Isl2 appears much more nociceptor specific than that of Isl1 (refs. 27,28), for which a role in nociceptor development and TrpV1 expression has been documented[24], although another report found broader RNA expression of Isl2 (ref. 45). Our results also raise questions as to why specific transcription factors facilitate or inhibit the reprogramming both to neuronal and nociceptor lineages. In contrast with prior studies[4,5,39], we found that Brn2 inhibited lineage reprogramming of mouse fibroblasts to neurons, and NeuroD1 decreased the efficiency and quality of human neurons. With regard to the nociceptor lineage, the roles of Brn3a and Klf7 in maintaining TrkA expression during embryonic development appear similar in the literature[22,25]. However, we found that Brn3a markedly inhibits lineage reprogramming to nociceptors, whereas Klf7 promotes it. Runx1, which is active and critical in the later embryonic stages of nociceptor development, does not facilitate the reprogramming process. Ngn1 has a well-characterized role in nociceptor development and eventual TrpV1 expression[21], but is involved much earlier in development (E9–13) than the other studied factors[20]. Thus, although developmental studies may inform the choice of transcription factors for lineage reprogramming, reprogramming studies may themselves provide insight into important developmental pathways and their regulators, recognizing of course that reprogramming may not recapitulate transcription factors expressed in normal development.

The intricacy and specificity of primary nociceptor neuron physiology and the fortunate ability to culture adult primary sensory neurons provide an unusual and well-controlled opportunity to evaluate how closely lineage-reprogrammed neurons resemble the molecular expression, function and maturity of primary adult neurons. We found that the reprogrammed neurons produced functional TrpV1, TrpA1 and TrpM8-expressing neurons in similar relative percentages to those found in primary tdTomato-positive adult mouse nociceptors. In addition, the induced neurons yielded not only functional TTX-resistant action potentials, but also the broad action potential morphology and phasic firing pattern characteristic of nociceptors. Indeed, their function globally was markedly close to that of adult primary nociceptors by every measure we made, although we cannot exclude other contributions, such as neuronal maturity, to firing pattern and action potential morphology. Future studies will need to explore the synaptic capacity, neurotrophin dependence and requirement for sustained viral transgene expression in the derived nociceptors.

Patient-derived neurons would have optimal utility as a drug screening tool if the derived neurons replicate the sequence of pathophysiological events that result in specific clinical diseases. Reprogrammed nociceptors may be particularly useful as an *in vitro* model for pain, as the pain-sensitization process mimicked by the induced nociceptors is one of the major factors that drive the transition to pathological pain. The development of a fluorescent nociceptor-specific marker will enable further optimization of human induced nociceptor maturation as well as more extensive molecular and physiological characterization of the human neurons. Whether nociceptors reprogrammed from individuals with chronic pain or peripheral neuropathy will reveal phenotypic differences compared with control subject–derived nociceptors can be evaluated in the future.

Analysis of FD patient tissue samples[40,41] and FD induced pluripotent stem cell–derived neural precursors[42] have consistently shown the presence of both abnormally and normally spliced transcripts in the same sample. The detection of both splice forms could reflect either the presence of both normal and aberrant splicing in the affected neuronal types or simply the heterogeneity of affected and unaffected tissue types in the samples. Our finding that the normal *IKBKAP* splice variant was apparently absent in the FD-derived neurons indicates that the latter is likely the case, may have implications regarding the extent of splice correction necessary for disease treatment and may explain the observation in a mouse FD model that small amounts of IKAP are sufficient to revert the phenotype[46]. The reduction in outgrowth and branching in familial dysautonomia compared with control-derived neurons may reflect the presence of processes similar to those responsible for the progressive decrease in unmyelinated sensory neurons that is observed clinically[40] and the loss of TrkA-positive neurons in a mouse model[47]. The ability to obtain FD nociceptors from patient fibroblasts will allow future studies to examine the mechanisms of disease and to screen and evaluate potential treatments. Our results illustrate how derived neurons with major features of primary nociceptors can be generated and employed as a model for 'pain in a dish'.

Note Added in Proof: Blanchard *et al.* in this issue used a similar lineage reprogramming strategy and also obtained neurons with molecular and physiological properties that spanned different sensory neuron subtypes.

METHODS

Methods and any associated references are available in the online version of the paper.

Note: Any Supplementary Information and Source Data files are available in the online version of the paper.

ACKNOWLEDGMENTS

We thank M. Costigan for assistance with RT-PCR, A. Yekkirala and J. Sprague for help with calcium imaging, Q. Ma (Dana-Farber Cancer Institute) and E. Turner (Seattle Children's Research Institute) for constructs, J. Gardner and J. McNeish for helpful advice and support, and K. Wainger for assistance with figure preparation. We also thank the Boston Children's Hospital IDDRC Molecular Genetics Core Facility for RNA Bioanalyzer analyses and the Harvard Medical

School ICCB Screening Facility for assistance with ImageXpress and MetaXpress analyses. This research was supported by the National Institute of General Medical Sciences (T32 GM07592) and National Institute of Neurological Disorders and Stroke (1K08-NS082364) to B.J.W. Conselho Nacional de Desenvolvimento Científico e Tecnológico (J.T.O.), GlaxoSmithKline Regenerative Medicine DPU (C.J.W.), the National Institute of Neurological Disorders and Stroke (NS038253 to C.J.W.), and the Dr. Miriam and Sheldon G. Adelson Medical Foundation (C.J.W.).

AUTHOR CONTRIBUTIONS

B.J.W. conceived, designed and performed the lineage reprogramming experiments and physiological experiments, analyzed data, and wrote the manuscript. E.D.B. designed, performed and analyzed reprogramming, quantitative PCR, single-cell RT-PCR, immunohistochemistry and CGRP ELISA experiments, and wrote the manuscript. J.T.O. performed and optimized the induced nociceptor technique. C.M. performed and analyzed physiological studies and edited the manuscript. S.L. performed CGRP ELISA and single-cell RT-PCR assays. W.A.S. performed reprogramming and immunohistochemistry experiments. A.J.W. performed initial cloning and transduction experiments. J.K.I. provided essential advice for nociceptor reprogramming strategy and edited the manuscript. I.M.C. gave critical advice regarding the genetic reporter, choice of transcription factors, performed cell sorting experiments and edited the manuscript. L.B. advised and performed molecular biology experiments. E.A.H. performed image quantification and analysis. C. Bilgin assisted with reprogramming and immunohistochemistry. N.T. assisted with human motor neuron culture and, together with C. Brenneis performed culture and characterization using initial approaches. K.K. performed statistical modeling of human nociceptor data. L.L.R. advised regarding reprogramming experiments and edited the manuscript. K.E. provided advice and reagents for reprogramming and edited the manuscript. C.J.W. designed experiments, interpreted findings and wrote the manuscript.

COMPETING FINANCIAL INTERESTS

The authors declare no competing financial interests.

1. Qiang, L., Fujita, R. & Abeliovich, A. Remodeling neurodegeneration: somatic cell reprogramming-based models of adult neurological disorders. *Neuron* **78**, 957–969 (2013).
2. Sandoe, J. & Eggan, K. Opportunities and challenges of pluripotent stem cell neurodegenerative disease models. *Nat. Neurosci.* **16**, 780–789 (2013).
3. Liu, M.L. *et al.* Small molecules enable neurogenin 2 to efficiently convert human fibroblasts into cholinergic neurons. *Nat. Commun.* **4**, 2183 (2013).
4. Vierbuchen, T. *et al.* Direct conversion of fibroblasts to functional neurons by defined factors. *Nature* **463**, 1035–1041 (2010).
5. Son, E.Y. *et al.* Conversion of mouse and human fibroblasts into functional spinal motor neurons. *Cell Stem Cell* **9**, 205–218 (2011).
6. Costigan, M., Scholz, J. & Woolf, C.J. Neuropathic pain: a maladaptive response of the nervous system to damage. *Annu. Rev. Neurosci.* **32**, 1–32 (2009).
7. Basbaum, A.I., Bautista, D.M., Scherrer, G. & Julius, D. Cellular and molecular mechanisms of pain. *Cell* **139**, 267–284 (2009).
8. Blair, N.T. & Bean, B.P. Roles of tetrodotoxin (TTX)-sensitive Na+ current, TTX-resistant Na+ current, and Ca2+ current in the action potentials of nociceptive sensory neurons. *J. Neurosci.* **22**, 10277–10290 (2002).
9. Chambers, S.M. *et al.* Combined small-molecule inhibition accelerates developmental timing and converts human pluripotent stem cells into nociceptors. *Nat. Biotechnol.* **30**, 715–720 (2012).
10. Waxman, S.G. Channelopathic pain: a growing but still small list of model disorders. *Neuron* **66**, 622–624 (2010).
11. Huang, J. *et al.* Small-fiber neuropathy Nav1.8 mutation shifts activation to hyperpolarized potentials and increases excitability of dorsal root ganglion neurons. *J. Neurosci.* **33**, 14087–14097 (2013).
12. Han, C. *et al.* Nav1.7-related small fiber neuropathy: impaired slow-inactivation and DRG neuron hyperexcitability. *Neurology* **78**, 1635–1643 (2012).
13. Sorge, R.E. *et al.* Genetically determined P2X7 receptor pore formation regulates variability in chronic pain sensitivity. *Nat. Med.* **18**, 595–599 (2012).
14. Reimann, F. *et al.* Pain perception is altered by a nucleotide polymorphism in SCN9A. *Proc. Natl. Acad. Sci. USA* **107**, 5148–5153 (2010).
15. Pitchford, S. & Levine, J.D. Prostaglandins sensitize nociceptors in cell culture. *Neurosci. Lett.* **132**, 105–108 (1991).
16. Lopshire, J.C. & Nicol, G.D. Activation and recovery of the PGE2-mediated sensitization of the capsaicin response in rat sensory neurons. *J. Neurophysiol.* **78**, 3154–3164 (1997).
17. Anand, U., Otto, W.R. & Anand, P. Sensitization of capsaicin and icilin responses in oxaliplatin treated adult rat DRG neurons. *Mol. Pain* **6**, 82 (2010).
18. Lee, K.J. & Jessell, T.M. The specification of dorsal cell fates in the vertebrate central nervous system. *Annu. Rev. Neurosci.* **22**, 261–294 (1999).
19. Knecht, A.K. & Bronner-Fraser, M. Induction of the neural crest: a multigene process. *Nat. Rev. Genet.* **3**, 453–461 (2002).
20. Woolf, C.J. & Ma, Q. Nociceptors–noxious stimulus detectors. *Neuron* **55**, 353–364 (2007).
21. Ma, Q., Fode, C., Guillemot, F. & Anderson, D.J. Neurogenin1 and neurogenin2 control two distinct waves of neurogenesis in developing dorsal root ganglia. *Genes Dev.* **13**, 1717–1728 (1999).
22. Dykes, I.M., Lanier, J., Eng, S.R. & Turner, E.E. Brn3a regulates neuronal subtype specification in the trigeminal ganglion by promoting Runx expression during sensory differentiation. *Neural Dev.* **5**, 3 (2010).
23. Chen, C.L. *et al.* Runx1 determines nociceptive sensory neuron phenotype and is required for thermal and neuropathic pain. *Neuron* **49**, 365–377 (2006).
24. Sun, Y. *et al.* A central role for Islet1 in sensory neuron development linking sensory and spinal gene regulatory programs. *Nat. Neurosci.* **11**, 1283–1293 (2008).
25. Lei, L. *et al.* The zinc finger transcription factor Klf7 is required for TrkA gene expression and development of nociceptive sensory neurons. *Genes Dev.* **19**, 1354–1364 (2005).
26. Cavanaugh, D.J. *et al.* Restriction of transient receptor potential vanilloid-1 to the peptidergic subset of primary afferent neurons follows its developmental downregulation in nonpeptidergic neurons. *J. Neurosci.* **31**, 10119–10127 (2011).
27. Wu, C., Macleod, I. & Su, A.I. BioGPS and MyGene.info: organizing online, gene-centric information. *Nucleic Acids Res.* **41**, D561–D565 (2013).
28. Allen Institute for Brain Science. Allen Spinal Cord Atlas http://mousespinal.brain-map.org/ (2012).
29. Fornaro, M.. *et al.* Neuronal intermediate filament expression in rat dorsal root ganglia sensory neurons: an *in vivo* and *in vitro* study. *Neuroscience* **153**, 1153–1163 (2008).
30. Cavanaugh, D.J. *et al.* Trpv1 reporter mice reveal highly restricted brain distribution and functional expression in arteriolar smooth muscle cells. *J. Neurosci.* **31**, 5067–5077 (2011).
31. Bautista, D.M. *et al.* TRPA1 mediates the inflammatory actions of environmental irritants and proalgesic agents. *Cell* **124**, 1269–1282 (2006).
32. Chen, C.C. *et al.* A P2X purinoceptor expressed by a subset of sensory neurons. *Nature* **377**, 428–431 (1995).
33. Jarvis, M.F. *et al.* A-317491, a novel potent and selective non-nucleotide antagonist of P2X3 and P2X2/3 receptors, reduces chronic inflammatory and neuropathic pain in the rat. *Proc. Natl. Acad. Sci. USA* **99**, 17179–17184 (2002).
34. Dib-Hajj, S.D., Cummins, T.R., Black, J.A. & Waxman, S.G. Sodium channels in normal and pathological pain. *Annu. Rev. Neurosci.* **33**, 325–347 (2010).
35. Renganathan, M., Dib-Hajj, S. & Waxman, S.G. Na(v)1.5 underlies the 'third TTX-R sodium current' in rat small DRG neurons. *Brain Res. Mol. Brain Res.* **106**, 70–82 (2002).
36. Dib-Hajj, S.D. *et al.* Two tetrodotoxin-resistant sodium channels in human dorsal root ganglion neurons. *FEBS Lett.* **462**, 117–120 (1999).
37. Nagy, I., Urban, L. & Woolf, C.J. Morphological and membrane properties of young rat lumbar and thoracic dorsal root ganglion cells with unmyelinated axons. *Brain Res.* **609**, 193–200 (1993).
38. Emery, E.C., Young, G.T., Berrocoso, E.M., Chen, L. & McNaughton, P.A. HCN2 ion channels play a central role in inflammatory and neuropathic pain. *Science* **333**, 1462–1466 (2011).
39. Pang, Z.P. *et al.* Induction of human neuronal cells by defined transcription factors. *Nature* **476**, 220–223 (2011).
40. Slaugenhaupt, S.A. *et al.* Tissue-specific expression of a splicing mutation in the IKBKAP gene causes familial dysautonomia. *Am. J. Hum. Genet.* **68**, 598–605 (2001).
41. Cuajungco, M.P. *et al.* Tissue-specific reduction in splicing efficiency of IKBKAP due to the major mutation associated with familial dysautonomia. *Am. J. Hum. Genet.* **72**, 749–758 (2003).
42. Lee, G. *et al.* Modeling pathogenesis and treatment of familial dysautonomia using patient-specific iPSCs. *Nature* **461**, 402–406 (2009).
43. Woolf, C.J. Overcoming obstacles to developing new analgesics. *Nat. Med.* **16**, 1241–1247 (2010).
44. Davidson, S. *et al.* Human sensory neurons: membrane properties and sensitization by inflammatory mediators. *Pain* **155**, 1861–1870 (2014).
45. Li, Y. *et al.* Cloning and expression of a novel human gene, Isl-2, encoded a LIM-homeodomain protein. *Mol. Biol. Rep.* **34**, 19–26 (2007).
46. Dietrich, P., Alli, S., Shanmugasundaram, R. & Dragatsis, I. IKAP expression levels modulate disease severity in a mouse model of familial dysautonomia. *Hum. Mol. Genet.* **21**, 5078–5090 (2012).
47. George, L. *et al.* Familial dysautonomia model reveals Ikbkap deletion causes apoptosis of Pax3+ progenitors and peripheral neurons. *Proc. Natl. Acad. Sci. USA* **110**, 18698–18703 (2013).
48. Rebelo, S., Chen, Z.F., Anderson, D.J. & Lima, D. Involvement of DRG11 in the development of the primary afferent nociceptive system. *Mol. Cell. Neurosci.* **33**, 236–246 (2006).
49. Anderson, D.J. Lineages and transcription factors in the specification of vertebrate primary sensory neurons. *Curr. Opin. Neurobiol.* **9**, 517–524 (1999).
50. Cheng, L. *et al.* Tlx3 and Tlx1 are post-mitotic selector genes determining glutamatergic over GABAergic cell fates. *Nat. Neurosci.* **7**, 510–517 (2004).

ONLINE METHODS

Fibroblasts. *Trpv1-Cre*$^{+/-}$*::tdTomato*$^{+/-}$ transgenic mice were generated by crossing *Trpv1-Cre*$^{+/+}$ mice with *tdTomato*$^{+/+}$ reporter mice on a *C57Bl6* background (both from Jackson Laboratories). MEFs were harvested from *Trpv1::tdTomato* embryos, of either gender, at E12.5, passaged once and frozen at −120 °C. Human fibroblasts (all from Coriell Institute) were obtained from three HC subjects (GM00969, 2-year-old Caucasian female; GM03348, 10-year-old Caucasian male; GM00316, 12-year-old Caucasian male) and from three age-matched subjects with FD (GM04663, 2-year-old Caucasian female; GM04959, 10-year-old Caucasian female; GM04899, 12-year-old Caucasian female). The use of human lines was approved under the Boston Children's Hospital Institutional Review Board.

Viruses and transductions. Complimentary DNAs for the nine candidate factors (obtained from the Dana-Farber/Harvard Cancer Center DNA Resource Core except for Ngn1, Tlx3 and Runx1, which were obtained from Q. Ma at the Dana-Farber Cancer Institute) were each cloned into the pMXs retroviral expression vector modified to contain a WRE using Gateway technology (Invitrogen). 293T cells were co-transfected with individual viruses and pHDMG and pIKLMV packaging plasmids using Lipofectamine 2000 (Life Technologies). Media was changed to new DMEM (GIBCO), 20% (vol/vol) fetal bovine serum (FBS, Invitrogen) and 50 U ml^{-1} penicillin/streptomycin (CellGro) after 16 h. At that time, fibroblasts were thawed and plated on 24-well plates (25,000 cells per well), 6-well plates (150,000 cells per well), 35-mm dishes (150,000 cells per well) or p515A MEA probes (Alpha Med Scientific, 12,000 cells per MEA) that were previously coated with poly-D-lysine (Sigma), gelatin (Cell Signaling) and laminin (Sigma). Viruses were harvested 24 h later, concentrated approximately fivefold using Amicon ultra centrifugal filter units (Millipore) and applied to fibroblasts with 5 μg ml^{-1} polybrene (Sigma) (day 0, transduction). Cortical mouse glia obtained from P0–2 C57Bl6 mice were added on day 2 for all but the calcium-imaging experiments. Media was switched on day 4 to N3 media: DMEM/F-12 (GIBCO), N2 and B27 supplements (Life Technologies), glutaMAX (Invitrogen), penicillin/streptomycin, FGF (20 ng ml^{-1}, Millipore) with 5% FBS, along with the neurotrophic factors BDNF, CNTF and GDNF (R&D Systems) at 10 ng ml^{-1} each. The TGFβ inhibitor RepSox (7.5 μM, Millipore), which has been shown to improve survival of different neuronal types over long-term culture (J.K.I. and K.E., unpublished data), was added for calcium imaging and human transductions. Media was changed every 2 d, and on day 10, NGF was also added to the media (50 ng ml^{-1}, Invitrogen).

Immunohistochemistry. Cells were fixed with 4% paraformaldehyde, washed three times with 1× phosphate-buffered saline (PBS), incubated in blocking buffer (1% (vol/vol) Blocking Reagent (Roche), 0.5% BSA (vol/vol), 0.1% Triton X-100) for one hour at room temperature (20–23 °C) and stained with primary antibodies overnight at 4 °C in blocking buffer. The next day, the cells were washed three times with 1× PBS, stained with secondary antibodies for 1 h at room temperature (20–23 °C) and washed three times with 1× PBS before imaging, which was performed using the microscope setup described below.

Primary antibodies included mouse antibody to β tubulin III (Sigma T8660, 1:1,000, validated[51]), rabbit antibody to peripherin (Millipore AB1530, 1:800, validated[52]), rabbit antibody to TrpV1 (Alomone Labs ACC-030, 1:200, validated[53]), rabbit antibody to CGRP (Calbiochem/Millipore PC205L, 1:300, validated[54]), chicken antibody to neurofilament, heavy chain (Millipore AB5539, 1:1,000, validated[55]), mouse antibody to Nestin (Abcam ab6142, 1:500, validated[56]), mouse antibody to smooth muscle actin (Sigma A5228, 1:300, validated[57]), goat antibody to Sox1 (Santa Cruz #SC17317, 1:50, validated[58]), mouse antibody to Ki67 (Sigma P6834, 1:500, validated[59]). Secondary antibodies included goat antibody to chicken AlexaFluor 568 (Life Technologies A11041, 1:500), goat antibody to chicken AlexaFluor 488 (Life Technologies A11039, 1:500), goat antibody to mouse AlexaFluor 488 (Life Technologies A11029, 1:500 for β tubulin III, Nestin and Ki67; 1:300 for smooth muscle actin), goat antibody to mouse AlexaFluor 568 (Life Technologies A11031, 1:500 for β tubulin III, Nestin and Ki67; 1:300 for smooth muscle actin), goat antibody to rabbit AlexaFluor 488 (Life Technologies A11008, 1:500 for peripherin; 1:200 for TrpV1 and CGRP), goat antibody to rabbit AlexaFluor 568 (Life Technologies A11011, 1:500 for peripherin; 1:200 for TrpV1 and CGRP), donkey antibody to goat AlexaFluor 488 (Life Technologies A11055, 1:100).

Primary DRG culture. DRGs were dissected from adult *Trpv1-Cre::tdTomato* mice (12–13 weeks) into Hank's balanced salt solution (HBSS) (Life Technologies). DRG were dissociated in 1 μg ml^{-1} collagenase A plus 2.4 U ml^{-1} dispase II (enzymes, Roche Applied Sciences) in HEPES-buffered saline (Sigma) for 90 min at 37 °C and then triturated down to single-cell level using glass Pasteur pipettes of decreasing size. DRGs were the centrifuged over a 10% BSA gradient and plated on laminin-coated cell culture dishes (Sigma). DRGs were cultured 24 h in B27-supplemented neurobasal-A medium plus 50 ng ml^{-1} NGF (Invitrogen), 2 ng ml^{-1} GDNF (Sigma), 10 μM arabinocytidine (Sigma) and penicillin/streptomycin (Life Technologies).

Quantitative PCR. To compare expression levels of select genes in *Trpv1-tdTomato*–positive induced nociceptors, *Trpv1-tdTomato*–positive primary DRGs and *Trpv1-tdTomato* MEFs, individual tdTomato-positive neurons and fibroblasts were picked using a micropipette. RNA was harvested from sets of 50 cells with the RNeasy Micro Kit (Qiagen) and reverse transcribed with SuperScript VILO cDNA synthesis kit (Life Technologies). Quantitative PCR was completed using mouse-specific TaqMan Gene Expression Assays (Life Technologies) and the TaqMan Gene Expression Master Mix (Life Technologies). A minimum of two technical replicates for each of three biological replicates (independent cell collections) were completed for each gene.

Single-cell RT-PCR. Single human induced nociceptors were picked using individual patch pipettes and placed into Single Transcript Amplification (RT-STA) mixture from the CellsDirect One-Step qRT-PCR Kit (Life Technologies) using primers for normally and aberrantly spliced *IKBKAP*[39] and *GAPDH*. RT-STA reaction products were used for PCR using the same *IKBKAP* and *GAPDH* primers and the resulting products were run on 1% agarose gels.

Calcium imaging. Cells were loaded with Fura2-AM (10 μg ml^{-1}, Molecular Probes) by incubating at room temperature (20–23 °C) for 1 h and then destained for 15 min in saline. For primary DRGs from adult *Trpv1-Cre*$^{+/-}$*::tdTomato*$^{+/-}$ mice, cells were imaged after 24 h in culture using an identical protocol. Cells were imaged using a Nikon Eclipse Ti microscope with a Xenon lamp, Andor DL-604M camera and standard 340- and 380-nm filters controlled by a Ludl Mac6000 shutter using Nikon Elements software. Exposure times were 300–600 ms and images were taken every 3 s. 1 min of baseline imaging was recorded before the addition of the agonists, during which control vehicle was applied after 30 s (data not shown). Menthol (250 μM) was applied at 1 min, followed by mustard oil (100 μM) at 2 min, capsaicin (1 μM) at 3 min and finally KCl (40 mM) at 4 min. For Trp channel experiments, each agonist was applied for 20 s and then washed out with external solution. In the PGE2 sensitization experiments, capsaicin (300 nM) was applied for 20 s after 2 min of recording, followed immediately by PGE2 (1 μM) for two minutes, a conditioned capsaicin (300 nM) application for 20 s and KCl (40 mM) after 4.5 min. Analysis of tdTomato-positive cells was performed using custom Matlab (Mathworks) software to include cells that responded to KCl (1.5× baseline), had a stable baseline during control vehicle application and a response to agonist with an amplitude of at least 10% of baseline, with subsequent agonist responses required to be both at least 10% of initial baseline and 10% above a second baseline value obtained during the immediately preceding wash period.

CGRP ELISA. Induced nociceptors, BAM-derived neurons and primary DRGs were exposed to KCl (20, 40, 60 or 80 mM), capsaicin (0.1 μM) or vehicle for 10 min at 37 °C. The supernatants were collected and analyzed using the Rat CGRP Enzyme Immunoassay Kit (Bertin Pharma/Cayman Chemical, #589001). Plates were read at 405 nm for 0.1 s on a Wallac Victor^2 1420 Multilabel Counter (PerkinElmer), and data were analyzed using the Wallac 1420 Workstation.

MEA recording. *Trpv1-Cre*$^{+/-}$*::tdTomato*$^{+/-}$ MEFs were plated on poly-D-lysine/laminin-coated p515A probes (Alpha Med Scientific) at typical densities of 12,000 cells per probe, transduced with retroviruses and cultured for 4 weeks. Recordings from 64 extracellular electrodes were made using a Med64 (Alpha Med Scientific) MEA recording amplifier with a head stage that maintained a temperature of 37 °C. Data were sampled at 20 kHz, digitized and analyzed using Mobius software (Alpha Med Scientific) with a 2-kHz 9-pole Bessel low pass filter using a sodium-based extracellular solution: 135 mM NaCl, 5 mM KCl,

2 mM $CaCl_2$, 1 mM $MgCl_2$, 10 mM glucose, 10 mM HEPES 10, pH 7.4. The probes were recorded after the application of capsaicin (1 μM concentration) or mustard oil (100 μM), which were applied at a 10× concentration at the edge of the well (far from the electrodes). Three replicates for each agonist, capsaicin and mustard oil, were completed from two separate transductions. For oxaliplatin sensitization experiments, cells were treated with either 50 μM oxaliplatin or vehicle control for 10 min and then recorded for one minute during treatment with 300 nM capsaicin.

Patch electrophysiology. Whole-cell patch recordings were performed on induced tdTomato-positive nociceptors, derived from *Trpv1-Cre*$^{+/-}$*::tdTomato*$^{+/-}$ MEFs, 4–5 weeks post-transduction and assessed for responses to capsaicin and α,β-methylene ATP (30 μM, Sigma), total and TTX-resistant (300 nM, Sigma) sodium currents, HCN depolarizating current sags and action potentials. Whole-cell current-clamp and voltage-clamp recordings were performed using a Multiclamp 700B (Molecular Devices) at 21–23 °C. Data were sampled at 20 kHz and digitized with a Digidata 1440A A/D interface and recorded using pCLAMP 10 software (Molecular Devices). Data were low-pass filtered at 2 kHz. Patch pipettes were pulled from borosilicate glass capillaries on a Sutter Instruments P-97 puller and had resistances of 2–4 MΩ. The pipette capacitance was reduced by wrapping the shank with Parafilm and compensated for using the amplifier circuitry. Series resistance was 5–10 MΩ and compensated by at least 80%.

For voltage-clamp recordings, voltages were elicited by 200-ms depolarizing steps from a holding potential of −80 mV to test potentials ranging from −100 mV to 30 mV in 10 mV increments. Responses to capsaicin (1 μM) and α,β-methylene ATP (30 μM) were measured in voltage clamp at a holding potential of −80 mV. Electrode drift was measured at the end of each recording and was typically 1–2 mV. The potassium-based intracellular solution contained 150 mM KCl, 2 mM $MgCl_2$, 10 mM HEPES, 4 mM MgATP, 0.3 mM NaGTP, 10 mM Na_2PhosCr, 1 mM EGTA, pH 7.4. For isolation of voltage-gated sodium currents, internal KCl was replaced by CsCl to block potassium currents and 100 μM $CdCl_2$ was applied to block calcium currents. 300 nM TTX was used to block TTX-sensitive voltage-gated sodium channels. HCN currents were measured by sequential hyperpolarizing steps in current clamp with an increment of −10-pA steps.

Quantification of cell number, axon length and axonal branching. All quantifications of cell count and morphological properties were performed by a researcher blind to genotype and condition. Reprogramming efficiency and percentage of TrpV1::tdTomato-positive, Tuj1-positive, peripherin-positive and CGRP-positive neurons were determined using MetaXpress software. The number of TrpV1::tdTomato-positive (mouse, minimum of three wells from each of three separate transdifferentiations) and Tuj1-positive (human, minimum of 12 wells from each of three separate transdifferentiations) neurons was divided by the number of fibroblasts plated to calculate the reprogramming efficiency. Axon length and branching were quantified from the six age-matched human fibroblast lines (three HC and three FD) with images from eight wells (two transductions) and four wells (one transduction) of each line (20 wells total per line).

To quantify the number of TrpV1::tdTomato-positive neurons resulting from infection of different combinations of transcription factors, tdTomato-positive neurons were counted by hand in at least four separate wells for each condition from two separate transductions and averaged (**Fig. 1** and **Supplementary Fig. 4**). Given the variability of retroviral transductions with large numbers of viruses, we did not quantify experiments with transductions of 11–12 viruses at once (**Supplementary Fig. 3**). For comparison of five factors ± NeuroD1, images were taken of six wells of each condition from one transduction.

Statistical analyses. All tests are two-tailed using a significance threshold of 0.05. We used a Mann-Whitney *U* test to evaluate CGRP release after log transformation to equalize variance between groups (**Fig. 4h**). This gave a W statistic of 16 (4 assays per group) and a *P* value of 0.03. We used a paired *t* test to evaluate baseline and PGE2-sensitized capsaicin responses in the induced mouse nociceptors (**Fig. 5a**). This gave a T statistic of 4.61 with 20 degrees of freedom (21 cells) and a *P* value of 9.7×10^{-4}. For comparison of transdifferentiation efficiency using five versus six factors, we used an unpaired *t* test to compare the average number of cells per field in six wells per group and got a T statistic of 6.1 with 10 degrees of freedom and $P = 10^{-4}$ (**Supplementary Fig. 9**).

For morphological analyses of human HC- and FD-derived neurons, we performed analyses of cell number, axonal outgrowth and number of branches (**Fig. 6**). Distribution of cell number and number of branches were not normal (Shapiro-Wilk test). We looked at the distribution of all the measures graphically and found that they were approximately normal. Variance of cell number, axon outgrowth and number of branches were not different between HC- and FD-derived neurons (Levene test). Using random intercept model and taking matching of cell lines into account provided FD disease effect estimates (standard errors) compared with HC: −2.3 (1.5) cell numbers, $P = 0.2632$; −291.3 (32.6) μM axon outgrowth per cell, $P = 0.0123$; −3.3 (0.4) branches per cell, $P = 0.0165$. *Post hoc* analysis to compare individual lines was performed using Tukey-Kramer for the three pairs of lines. Comparisons of FD line 1 to matched HC line 1 gave estimate of differences as 2.1 (cells), −292.3 (outgrowth), −3.5 (branches), respectively. Comparisons of FD line 2 to matched HC line 2 gave estimate of differences as −7.2 (cells), −274.7 (outgrowth), −3.2 (branches), respectively. Comparisons of FD line 3 to matched HC line 3 gave estimate of differences as −1.9 (cells), −307.1 (outgrowth), −3.1 (branches), respectively. However, the model with interaction parameter for cell line type and disease group only provided generalized inverse estimates of the standard errors. Thus, the confidence intervals and *P* values for these individual cell lines are not reported. All statistical analyses were performed in software R version 3.1.0 and SAS ver 9.1. No power analyses were used to pre-determine sample sizes, but our sample sizes are similar to those used by others in the field.

A **Supplementary Methods Checklist** is available.

51. Banerjee, A., Roach, M.C., Trcka, P. & Luduena, R.F. Increased microtubule assembly in bovine brain tubulin lacking the type III isotype of beta-tubulin. *J. Biol. Chem.* **265**, 1794–1799 (1990).
52. Lysakowski, A., Alonto, A. & Jacobson, L. Peripherin immunoreactivity labels small diameter vestibular 'bouton' afferents in rodents. *Hear. Res.* **133**, 149–154 (1999).
53. Belghiti, M. *et al.* Potentiation of the transient receptor potential vanilloid 1 channel contributes to pruritogenesis in a rat model of liver disease. *J. Biol. Chem.* **288**, 9675–9685 (2013).
54. Maatkamp, A. *et al.* Decrease of Hsp25 protein expression precedes degeneration of motoneurons in ALS-SOD1 mice. *Eur. J. Neurosci.* **20**, 14–28 (2004).
55. Ghilardi, J.R. *et al.* Sustained blockade of neurotrophin receptors TrkA, TrkB and TrkC reduces non-malignant skeletal pain but not the maintenance of sensory and sympathetic nerve fibers. *Bone* **48**, 389–398 (2011).
56. Regad, T., Roth, M., Bredenkamp, N., Illing, N. & Papalopulu, N. The neural progenitor–specifying activity of FoxG1 is antagonistically regulated by CKI and FGF. *Nat. Cell Biol.* **9**, 531–540 (2007).
57. Skalli, O. *et al.* A monoclonal antibody against alpha-smooth muscle actin: a new probe for smooth muscle differentiation. *J. Cell Biol.* **103**, 2787–2796 (1986).
58. Panayi, H. *et al.* Sox1 is required for the specification of a novel p2-derived interneuron subtype in the mouse ventral spinal cord. *J. Neurosci.* **30**, 12274–12280 (2010).
59. Hoffmann, S. *et al.* Retinoic acid inhibits angiogenesis and tumor growth of thyroid cancer cells. *Mol. Cell. Endocrinol.* **264**, 74–81 (2007).

doi:10.1038/nn.3886